# Accurate Equilibrium Structures Obtained from Gas-Phase Electron Diffraction Data: Sodium Chloride

**Philip D. McCaffrey,[†] Richard J. Mawhorter,[‡] Andrew R. Turner,[†] Paul T. Brain,[†] and David W. H. Rankin*[,†]**

*School of Chemistry, University of Edinburgh, West Mains Road, Edinburgh EH9 3JJ, United Kingdom, and Department of Physics and Astronomy, Pomona College, 610 North College Avenue, Claremont, California 91711-6359*

*Received: May 1, 2007*

A novel method has been developed to allow the accurate determination of equilibrium gas-phase structures from experimental data, thus allowing direct comparison with theory. This new method is illustrated through the example of sodium chloride vapor at 943 K. Using this approach the equilibrium structures of the monomer (NaCl) and the dimer ($Na_2Cl_2$), together with the fraction of vapor existing as dimer, have been determined by gas-phase electron diffraction supplemented with data from microwave spectroscopy and ab initio calculations. Root-mean-square amplitudes of vibration ($u$) and distance corrections ($r_a - r_e$) have been calculated explicitly from the ab initio potential-energy surfaces corresponding to the vibrational modes of the monomer and dimer. These $u$ and ($r_a - r_e$) values essentially include all of the effects associated with large-amplitude modes of vibration and anharmonicity; using them we have been able to relate the $r_a$ distances from a gas-phase electron diffraction experiment directly to the $r_e$ distances from ab initio calculations. Vibrational amplitudes and distance corrections are compared with those obtained by previous methods using both purely harmonic force fields and those including cubic anharmonic contributions, and the differences are discussed. The gas-phase equilibrium structural parameters are $r_e(Na-Cl)_{monomer} = 236.0794(4)$ pm; $r_e(Na-Cl)_{dimer} = 253.4(9)$ pm; and $\angle_e ClNaCl = 102.7(11)°$. These results are found to be in good agreement with high-level ab initio calculations and are substantially more precise than those obtained in previous structural studies.

## Introduction

Knowledge of molecular structure is of vital importance to the understanding of chemical properties. Experimental and theoretical methods can independently provide significant insights into structure, but much more can be gained when the two are used together. Techniques, developed in Edinburgh, that allow this, such as SARACEN[1−3] and DYNAMITE,[4] have enabled accurate structural determinations that could not be carried out using experimental data alone.

Computational methods are now widely employed, often by non-experts, in all areas of chemistry, to give data for comparison with experimental results. However, where high accuracy is required, there is a fundamental flaw when making these comparisons: the definitions of structures obtained experimentally and by theory are inherently different.

To determine molecular structures accurately it is essential to define precisely the meanings of the geometrical parameters that are obtained. For example, X-ray diffraction (XRD) gives the position of the center of electron density for each atom, whereas neutron diffraction, electron diffraction, rotational spectroscopy, and NMR spectroscopy all give nuclear positions. Additionally, molecular vibrations can cause substantial differences between internuclear distances determined by different methods. In contrast, computational methods provide information about the multidimensional potential-energy surface (PES), with structures corresponding to minima on that surface. These are termed equilibrium structures ($r_e$) and correspond to the molecular geometry in theoretical vibrationless states.

For comparison with most computed structures, gas-phase structures are of particular value, as it is only in the gas phase that molecules are free from intermolecular forces that may distort their structures. The structures of these isolated molecules can then be compared directly with theory, assuming that vibrational motion can be accounted for. With the increased use of computational techniques in all areas of chemistry, computed structures play a vital role both in supplementing, and for comparison with, experimental data. At present, with materials and biological chemistry at the forefront of science, it is important to note that the parametrization of force fields used in molecular mechanics modeling programs is largely derived from experimental gas-phase structures. Gas-phase experimental structures that can be related directly to theory are therefore of vital importance to the further development of computational chemistry.

Microwave spectroscopy can provide very accurate geometrical and vibrational information and therefore yields very precise equilibrium structures using techniques such as the MORBID method.[5,6] However, the applicability of microwave spectroscopy is normally restricted to molecules with a permanent dipole moment, and often many isotopomers must be studied. Although other experimental techniques can give rotational constants, they are often substantially less precise. To obtain equilibrium structures for a much wider range of

[†] University of Edinburgh.
[‡] Pomona College.

10.1021/jp073328o CCC: $37.00 
Published on Web 06/19/2007

molecules, gas-phase electron diffraction (GED) is the technique of choice. However, this increase in the number of systems that can be studied comes at a price: GED does not provide the same accurate vibrational information that can be extracted from microwave spectroscopy, making the determination of equilibrium structures much more difficult. Traditional methods involve using a harmonic force field derived from either theory or experiment to provide corrections for vibrational motion, which are then applied to the experimental structure. Unfortunately, these corrections can sometimes introduce errors larger than those they are designed to correct, because the effects of both anharmonicity and large-amplitude vibrations are not normally included.

There are three fundamental problems associated with calculating vibrational correction terms using the current approach: (1) extrapolation of information that relates solely to the bottom of the potential-energy well, which is especially relevant for systems involving large-amplitude modes of vibration; (2) nonlinear motion of atoms; and (3) effects arising from anharmonicity.

A more realistic description of the nonlinear motions of atoms can be obtained by using curvilinear corrections,[7,8] as opposed to the traditional rectilinear modeling of atomic motion.[9,10] Although an improvement, this approach remains reliant on a harmonic force field computed at the equilibrium geometry and will inaccurately describe large-amplitude modes and modes involving unusual motions such as restricted torsions.

Problems associated with anharmonic effects can be tackled by the computation of anharmonic force fields,[11] which include higher-order terms than those in harmonic force fields, to give a better description of the shape of the PES in the vicinity of the equilibrium structure. Software that can include some form of cubic anharmonicity in vibrational correction terms has been developed.[12] However, methods giving a full anharmonic treatment are still far from routine. In addition, these methods continue to rely on the extrapolation of information determined from the equilibrium position and thus remain inadequate for large-amplitude modes of vibration.

Our novel approach, EXPeriments Resulting in Equilibrium StructureS (EXPRESS) accounts for all three of these problems simultaneously, by exploring a much more extensive region of the PES, specifically along internal coordinates relating to the vibrational modes of the molecule. This allows the single-step computation of vibrational corrections relating the vibrationally averaged GED distances ($r_a$) to equilibrium distances ($r_e$); the result is an equilibrium structure determined directly from experimental data. The alkali halide dimers, present in the vapor phase, provide excellent test cases for this procedure: they are simple, floppy molecules that contain low-frequency modes of vibration that are both anharmonic and of large amplitude.

**Sodium Chloride.** Sodium chloride was chosen as the test case for the EXPRESS method. The vapor contains both monomer and dimer species at the temperatures required for electron diffraction. The use of very high temperatures (approximately 1000 K) results in vibrational corrections being relatively large and thus very important for accurate structure determination. The dimer has low-frequency modes of vibration, and so high vibrational states are highly populated at these temperatures. In particular, it has a low-frequency, large-amplitude bending vibration that is inadequately modeled by current methods. Furthermore, it is particularly convenient that the six modes of vibration are of five different symmetry species; this limits the degree of coupling between the different vibrational modes, so it is straightforward to see the effects of our method of analysis.

Sodium chloride is the classic example of ionic bonding, and accurate structures can provide a critical test for various models, resulting in better understanding of this type of bonding. Moreover, the dimer is the first step from monomers to larger clusters. Ionic models[13] have often been used to study these transitional structures. Examples of more recent work in this area include an electron-diffraction study of specific CsI clusters,[14] work on the dynamic isomerization of small cesium halide cluster anions,[15] and the observation and manipulation of NaCl chains on a copper surface.[16]

The determination of the structure of sodium chloride vapor by GED dates back as far as 1937,[17] when it was studied by heating salt to around 1000 K. As a consequence of the visual analysis methods in use at the time, only the predominant and expected monomer species was detected. It was not until the 1950s that the existence of associated species such as dimers ($Na_2Cl_2$) were discovered using mass spectrometry.[18] Microwave spectroscopy has provided detailed information on the structure of the monomer,[19−21] but the lack of a permanent dipole moment makes this impossible for the dimer.

Experimental difficulties made accurate study of the dimer very demanding, and so it was not until 1985 that its structure could be determined by electron diffraction.[22] Nevertheless, this study was hindered by the fact that almost all of the parameters are strongly correlated. The monomer and dimer bonded distances are similar and cannot easily be resolved, because of the large amplitude of the stretching vibrations at high temperature. The proportion of dimer present in the vapor is also strongly correlated to these distance parameters. Since the first publication of the results of this study, there has been much progress in the treatment of vibrational effects in electron diffraction. Although current techniques provide a significant improvement on previous methods, the floppy nature of the dimer illustrates the limitations of these methods in capturing the vibrational behavior correctly and thus to derive the equilibrium structure. These problems result from the high degree of anharmonicity in the vibrational modes as well as from the large-amplitude mode of vibration combined with the significant population of higher vibrational states. By using our much-improved vibrational correction terms, introducing highly accurate data obtained by microwave spectroscopy to restrain the monomer distance using the STRADIVARIUS method[23] and applying flexible restraints to amplitudes that prove problematic to refine using the SARACEN method,[1−3] the problems of previous studies have been overcome.

## Theory

**Definition of Vibrational Correction Terms.** The diffraction equations governing electron scattering relate the scattering intensities to interatomic distances. Consequently, the distance obtained directly from electron diffraction ($r_a$) is defined by eq 1, where the averaging is over all vibrational modes.

$$r_a = \langle r^{-1} \rangle^{-1} \tag{1}$$

Traditionally, the approach by which we can relate these averaged structures ($r_a$), obtained from electron diffraction, to equilibrium structures ($r_e$), calculated from theoretical methods, proceeds as follows. First, the inverted averaged inverse distance, $r_a$, can be related to the thermally averaged distance, $r_g$, by eq 2,

$$r_g \equiv \langle r \rangle = r_a + \frac{u^2}{r_e} \quad (2)$$

where the *u* term is the root-mean-square (RMS) amplitude of vibration for the atom pair. This correction is relatively small and so the fact that $r_e$ is used in the correction term is not significant, and in practice $r_a$ is often used in its place.

The distance between average nuclear positions in the ground vibration state when $T = 0$ K ($r_\alpha^0$) can be derived from $r_g$ by accounting for motion of the atoms perpendicular to the interatomic vector, which can cause apparent shortening or lengthening of interatomic distances. These motions generally contribute to the overall shortening of nonbonded distances, which is known in electron diffraction as the "shrinkage effect".[24−26] This is achieved by the subtraction of a further correction term, *k*, and also an anharmonic term, $A_T - A_0$, which is difficult to evaluate.

$$r_\alpha^0 = r_g - k - (A_T - A_0) \quad (3)$$

Typically the *k* term is generated in the harmonic approximation, and the anharmonic term is usually small and is often ignored. Distances derived this way are labeled $r_{hn}$, where h implies a harmonic correction and *n* indicates the level of the correction term, that is, 0 indicates a zeroth-order correction, 1 indicates a first-order correction, and so forth. It is important to note at this point that the parameter $r_\alpha^0$ has a fundamental, precisely defined physical meaning (the distance between average nuclear positions when $T = 0$ K) and that experimental distances quoted as $r_\alpha^0$ are usually approximations to it, and in most cases are in fact $r_{h0}$ distances. It is also important to note that $r_\alpha^0$ is equivalent to $r_z$ obtained from rotational constants; they are just obtained by different methods.

The remaining difference between $r_\alpha^0$ and $r_e$ depends on a further anharmonic term, as shown in eq 4.

$$r_e = r_\alpha^0 - A_0 \quad (4)$$

The anharmonic terms in the above equations are difficult to evaluate accurately, but to assess their magnitude pairs of atoms are often treated as diatomic molecules using a Morse potential. In this case, the cubic anharmonic term ($A_{3,T}$) is given by eq 5, where $a_3$ is the Morse anharmonic constant and *u* is the amplitude of vibration. Approximate values for $A_T$ and $A_0$ are thus obtained from the amplitude of vibration at the temperature of the experiment ($u_T$) and at 0 K ($u_0$), respectively.

$$A_3 = \frac{3a_3u(T)^2}{2} \quad (5)$$

In all cases distortion of the structure resulting from rotation must also be taken into account. This can be accounted for by subtraction of a further correction term arising from the centrifugal distortion ($\delta r$), which is usually relatively small.

The required distance correction terms mentioned above are routinely calculated from a harmonic force field hence, and anharmonic effects are neglected. This may be obtained from experimental vibrational frequencies and other data, computed ab initio, or based on force constants from similar molecules. In these cases the *k* correction term proves the most cumbersome to compute. At the zeroth level of approximation (giving a $r_{h0}$ structure), it is assumed that the atomic motions are described by rectilinear paths, that is, atomic displacements from equilibrium are in straight lines. This is described by Wilson et al.[27]

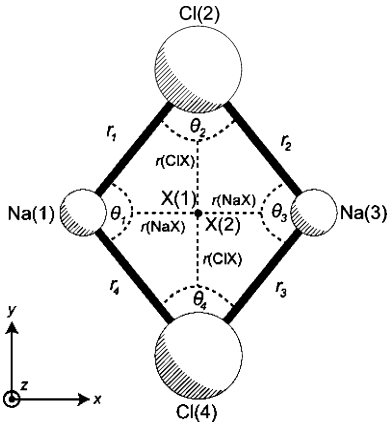


**Figure 1.** Structure of the $Na_2Cl_2$ dimer.

and is implemented in the program ASYM.[9,10] Treating molecular vibrations using rectilinear motions assumes implicitly that the motion simply follows the original displacements calculated at equilibrium, no matter how great the amplitude of vibration. This is a convenient way to model very small-amplitude modes of vibration, but a moment's consideration of the bending motion of a linear triatomic molecule serves to illustrate that this approach can be seriously inaccurate. The next level of approximation ($r_{h1}$), as realized in the SHRINK program,[7,8] provides a better (curvilinear) description of molecular motion, but many large-amplitude vibrations are still not described accurately. As a result, the *k* correction terms can often be very inaccurate and can sometimes introduce errors larger than those that they are trying to correct! Furthermore, anharmonic effects are not included in either of these approaches because the correction terms are generated using harmonic force fields. However, SHRINK can provide an estimate of cubic anharmonic effects from either tabulated constants for the two atoms or, more accurately, using third derivatives of the energy.

## Method and Experiment

**Theoretical Calculations.** Extensive series of calculations were performed on both the monomer and the dimer to assess the effect of computational method and basis set on the structural parameters and to provide the most accurate equilibrium structure possible for comparison with experimental results. The vast majority of calculations were performed on a 12-processor Parallel Quantum Solutions (PQS) workstation running the Gaussian 03 suite of programs.[28] Møller−Plesset (MP2)[29−34] and coupled cluster [CCSD(T)][35−41] calculations with basis sets larger than triple ζ were performed using the resources of the EPSRC National Service for Computational Chemistry Software[42] on a cluster of 22 dual Opteron compute servers. Each Opteron compute machine has two 2.4 GHz Opteron 250 CPUs and 8 GB of memory. These are connected with a high-speed, low-latency Myrinet network. For all of the calculations the convergence criteria were tightened to 1.236 pN, 0.741 pN, 3.175 fm, and 2.117 fm for the maximum force, RMS force, maximum displacement, and RMS displacement, respectively. This was to ensure consistency between the energies of equilibrium structures and those calculated using the modes of vibration.

**Calculation of Vibrational Correction Terms.** For the purposes of this study, the *z*-axis was defined to be through the center of the dimer, perpendicular to the plane of the molecule, and the *x*-axis through the two metal atoms (as shown in Figure 1). This allows the symmetry species of the modes of vibration to remain consistent for all the alkali halides, allowing for any

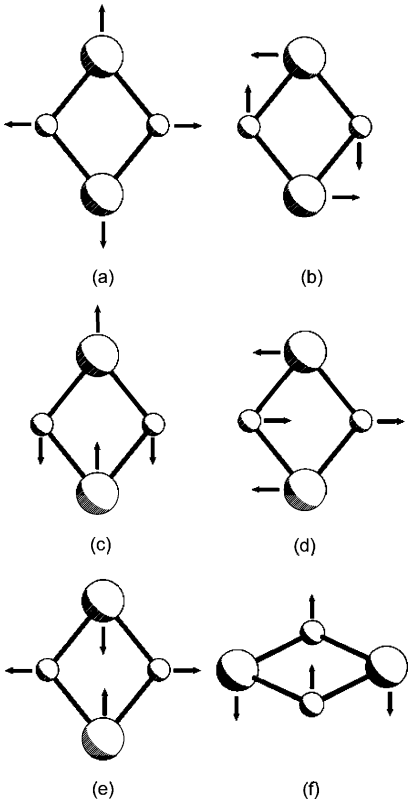


**Figure 2.** Vibrational modes of the $Na_2Cl_2$ dimer. Stretching modes (a) $A_g$, (b) $B_{1g}$, (c) $B_{2u}$, and (d) $B_{3u}$; bending modes (e) $A_g$ and (f) $B_{1u}$.

**TABLE 1: Parameters Used To Model Vibrational Modes**[a]

| mode | | fixed parameter | internal coordinate ($\rho$) |
|---|---|---|---|
| | | Monomer | |
| $A_1$ stretch | stretch | $r$ | $r$(Na−Cl) |
| | | Dimer | |
| $A_g$ stretch | symmetric stretch | $r_1 (=r_2 = r_3 = r_4)$ | $r$(Na−Cl) |
| $B_{1g}$ stretch | asymmetric stretch | $r_1 (=r_3) - r_2 (=r_4)$ | $r$[X(1)−X(2)] |
| $B_{2u}$ stretch | asymmetric stretch | $r_1 (=r_4) - r_3 (=r_2)$ | $r$[X(1)−X(2)] |
| $B_{3u}$ stretch | asymmetric stretch | $r_1 (=r_2) - r_4 (=r_3)$ | $r$[X(1)−X(2)] |
| $A_g$ bend | in-plane bend | $\theta_1 (=\theta_3) - \theta_2 (=\theta_4)$ | ∠(Na−Cl−Na) |
| $B_{1u}$ bend | out-of-plane bend | 4-membered ring pucker | $r$[X(1)−X(2)] |

[a] For the definitions of the parameters see Figure 1.

future comparisons. The monomer species (NaCl) has one mode of vibration of $A_1$ symmetry and the dimer ($Na_2Cl_2$) has six modes of vibration, of five different symmetry species, $2A_g + B_{1g} + B_{1u} + B_{2u} + B_{3u}$. The natures of the vibrational modes for the dimer are illustrated in Figure 2. The RMS amplitudes of vibration ($u$) and explicit distance corrections ($r_a - r_e$) were calculated using the EXPRESS method as detailed below.

A harmonic force field computed at the MP2(full)/6-311+G(d)[43−46] level, including electron correlation for all electrons, was used to generate atomic displacements in the first approximation. Although a low-level force field could be used, as it is simply required to provide a rough description of the modes, a higher-level force field was used in this case. This enabled distance corrections calculated from it (using traditional methods) to be compared with those obtained by our EXPRESS method.

An internal coordinate ($\rho$) was then chosen to represent each mode of vibration. These are listed in Table 1. Values of the chosen internal coordinate were then selected to represent the range of vibration, with energies ranging up to at least 5 kT. More values were taken around the equilibrium position as these have a higher probability of occupation.

For each mode, the structure was then re-optimized at the MP2(full)/6-311+G(d) level with the one selected geometrical parameter ($\rho$) fixed at the values chosen in the previous step, while allowing all the other parameters to relax. Energies and atomic coordinates were recorded for each optimization. In this way we produced one-dimensional (1D) slices through the multidimensional PES, corresponding to the minimum potential-energy path for each particular vibrational mode.

For each 1D PES slice, the calculated energy was fitted using an appropriate function of the internal coordinate (a Morse potential, or a harmonic, or higher-order polynomial as required). The variation of the interatomic distances ($ij$), Na−Cl, Na···Na, and Cl···Cl, corresponding to the 1D PES slice, were then also fitted to similar analytical expressions.

Contributions from each of the $n$ modes ($m$) to terms $u_{ij}$, $(r_a - r_e)_{ij}$, $(r_a - r_g)_{ij}$, and so forth, were then calculated by integration, using the Boltzmann distribution to give populations over the occupied energy range at the temperature of the experiment, in accord with eqs 6 and 7,

$$u_{ij}^m = \left( \frac{\int (r_{ij} - r_{e,ij})^2 P(r)\, \delta r}{\int P(r)\, \delta r} \right)^{1/2} \tag{6}$$

$$(r_a - r_e)_{ij}^m = \left( \frac{\int r_{ij}^{-1} P(r)\, \delta r}{\int P(r)\, \delta r} \right)^{-1} - r_{e,ij} \tag{7}$$

where

$$P(r) = \exp\left(\frac{-E}{kT}\right)$$

Contributions from the individual modes were then combined to give the overall vibrational correction terms, using the scheme given in eqs 8 and 9.

$$u_{ij} = \left( \sum_{m=1}^{n} (u_{ij}^m)^2 \right)^{1/2} \tag{8}$$

$$(r_a - r_e)_{ij} = \sum_{m=1}^{n} (r_a - r_e)_{ij}^m \tag{9}$$

The experimental data utilized in this study were obtained at 943 K, which corresponds to a thermal energy of 7.84 kJ mol$^{-1}$.

For this system only one internal coordinate was chosen to represent each mode of vibration (i.e., we explored only a 1D potential-energy curve). For more complex systems with multiple, coupled large-amplitude or very anharmonic vibrational modes, it may be necessary to perform the analysis on multidimensional PESs.

The modeling parameter (internal coordinate) was chosen to be independent of all the other vibrational coordinates. To model each of the modes accurately, all of the remaining parameters were relaxed, thus producing the minimum 1D PES slice corresponding to the vibrational motion on the multidimensional PES. The parameters chosen to represent each of the vibrational modes are shown in Table 1. For the monomer and for the symmetric stretch of the dimer, the chosen parameter ($\rho$) was simply the bonded distance and was contracted and expanded as in the scheme previously defined. To aid the modeling of the other vibrational modes of the dimer, two dummy atoms

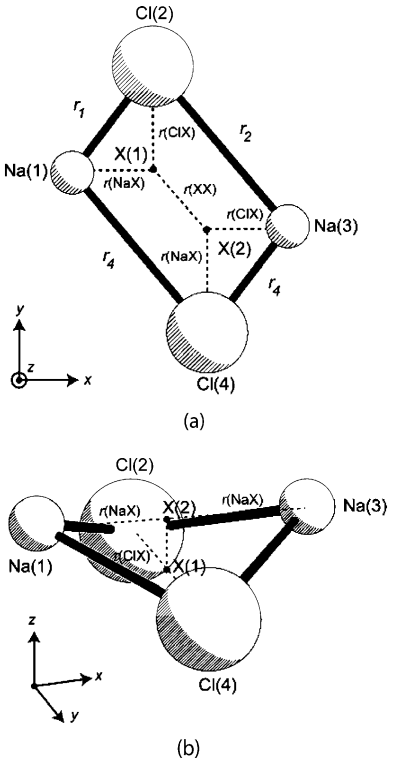


**Figure 3.** Scheme for modeling vibrational modes: (a) $B_{1g}$ stretch and (b) $B_{1u}$ bend.

[X(1) and X(2)] were defined, originating midway between Na(1)···Na(3) and Cl(2)···Cl(4), respectively, as shown in Figure 1. For the $B_{1g}$ symmetric stretch, the atoms Na(1) and Cl(2) were attached to dummy atom X(1), and Na(3) and Cl(4) were attached to dummy atom X(2). The distance between the two dummy atoms was then varied along the line $x = -y$, as shown in Figure 3a. Thus the individual bond lengths and angles could be optimized but the difference between $r_1$ and $r_2$ (equivalent to $r_3$ and $r_4$) remained fixed.

A similar principle was applied to all the other modes. The model for the $B_{2u}$ asymmetric stretch was implemented by attaching Na(1), Cl(2), and Na(3) to X(1) and Cl(4) to X(2). The distance between the two dummy atoms was then varied along the *y*-axis. For the $B_{3u}$ mode, Na(1), Cl(2), and Cl(4) were attached to X(1) and Na(3) was attached to X(2), with the distance between the two dummy atoms being varied along the *x*-axis. The in-plane $A_g$ bending motion was modeled by fixing the Na(1)−Cl(2)−Na(3) and Na(3)−Cl(4)−Na(1) angles while letting the bonded distance be refined. Finally, the out-of-plane $B_{1u}$ bending motion involved attaching the two chlorine atoms to X(1) and the two sodium atoms to X(2) and then varying the X(1)−X(2) distance in the *z* direction, as shown in Figure 3b. This is a similar scheme to the one utilized by Laane to model a four-membered ring pucker.[47]

**Gas-Phase Electron Diffraction (GED).** The data used for this study are those obtained by Mawhorter et al.[22] The sample of sodium chloride used was commercially available and of 99.97% purity. An accelerating voltage of approximately 41.5 keV was used, and the precise electron wavelength was determined by using the standard $r_a$(C−O) value for $CO_2$ of 116.42 pm. Scattering intensities were determined by counting electrons at each angle for 300 s. These were then averaged in intervals of 2 $nm^{-1}$ from $s = 40$ to 178 $nm^{-1}$.

The weighting points for the off-diagonal weight matrix, correlation parameters, and scale factors for the data are given in Table S1 (Supporting Information). Further data reduction and the least-squares refinements were then carried out using the *ed@ed* structural refinement program[48] using the scattering factors of Ross et al.[49]

## Results and Discussion

**Theoretical Calculations: Equilibrium Geometry.** There are many examples of ab initio and density functional theory (DFT) studies of sodium chloride in the literature.[50−54] It seems that there is great difficulty in reproducing the highly accurate experimental equilibrium structure for the monomer obtained by microwave spectroscopy. One of the main problems involves the electron-correlation method. As a result of unfavorable scaling of electron-correlation schemes, it is usually the case that electrons are partitioned into inner-shell core electrons and "chemically relevant" valence electrons. Unfortunately, the electronic configuration of sodium ($1s^2 2s^2 2p^6 3s^1$) dictates that standard electron-correlation schemes (using a frozen-core methodology) would only include correlation for the single 3s electron. This approach is clearly inappropriate, especially in a highly ionic system such as sodium chloride.

An extensive range of calculations was performed at various levels of theory and with different basis sets to gauge their effect on the structures of the monomer and dimer species. Thus, we were able to determine a method and basis set that could be used to model the vibrational modes while keeping the computational cost at a reasonable level. High-level theory calculations were also performed to try to obtain the best possible description of the monomer and dimer for comparison with experimental results. Table 2 gives results from various calculations of the equilibrium structure ($r_e$) of both the monomer and the dimer together with prominent results from the literature.

The results using the 6-311+G(d) basis set show a shortening of the Na−Cl distance for both the monomer and the dimer (by approximately 1.6 and 3.4 pm, respectively) on the addition of the standard frozen-core electron correlation. Increasing the sophistication of the correlation from MP2 to the CCSD(T) has little effect on the geometries. However, increasing the correlation to include core electrons has a marked effect on the distances, leading to a further decrease of 0.6 pm for the monomer and 0.9 pm for the dimer. Again, the sophistication of the correlation method has little effect. The Cl−Na−Cl angle in the dimer remains reasonably consistent throughout all levels of theory, with a slight decrease of around 0.5° when only valence correlation is included.

The results using the 6-311+G(d) basis set show that inclusion of the core electrons in the correlation scheme has a much larger impact on the structures of both the monomer and the dimer than the sophistication of the scheme itself. As long as some form of electron correlation is included, the difference between the monomer and the dimer is reasonably consistent.

For the monomer, using the highest level of theory [CCSD(T)] and the 6-311+G(d) basis set, the results still give a discrepancy of 1.6 pm between theory and experiment for the monomer. This suggests that the basis set is not accurately describing the bonding.

Calculations on alkali halide−rare gas clusters by Lee and Lee[55] showed the importance of core correlation but also indicated that it was necessary to include polarization functions with higher angular momentum, using the 6-311+G(3df) basis set. In the case of sodium chloride, this had no effect on the monomer distance but increased the dimer distance by 0.6 pm and increased the angle by a degree. The Dunning style correlation-consistent polarized basis sets (cc-pV*n*Z) give very

**TABLE 2: Calculated Geometries ($r_e$) for Both Monomer and Dimer at Different Levels of Theory[a]**

| theory/basis set | $r_e(Na-Cl)_{monomer}$ | $r_e(Na-Cl)_{dimer}$ | $\angle_e(Cl-Na-Cl)$ | $r_e(Na-Cl)_{difference}$ |
|---|---|---|---|---|
| RHF/6-311+G(d) | 239.8 | 257.3 | 101.0 | 17.5 |
| MP2/6-311+G(d)[b] | 238.2 | 253.9 | 100.5 | 15.7 |
| CCSD(T)/6-311+G(d)[b] | 238.3 | 253.9 | 100.7 | 15.7 |
| MP2(full)/6-311+G(d)[c] | 237.6 | 253.0 | 100.9 | 15.4 |
| CCSD(T)(full)/6-311+G(d)[c] | 237.7 | 253.0 | 101.1 | 15.3 |
| MP2(full)/6-311+G(3df)[c] | 237.6 | 253.6 | 101.8 | 16.0 |
| MP2(full)/cc-pVTZ[c] | 237.4 | 254.3 | 103.0 | 16.9 |
| MP2(full)/cc-pVQZ[c] | 238.6 | 246.3 | 132.3 | 7.7 |
| MP2(full)/aug-cc-pVQZ[c] | 229.0 | 244.8 | 118.3 | 15.8 |
| MP2(full)/CVQZ/cc-pCVQZ[c] | 236.8 | 253.3 | 101.8 | 16.6 |
| RHF/TZP[d] | 238.9 | 257.1 | 101.6 | 18.2 |
| RHF/ECP[e] | 239.7 | 258.0 | 100.8 | 18.3 |
| RHF/POL[f] | 240.0 | 257.4 | 100.8 | 17.4 |
| CPF/TZP[d] | 236.1 | 252.8 | 101.8 | 16.7 |
| MP2/POL[f] | 238.4 | 253.8 | 100.2 | 15.4 |
| DFT/DZP[g] | 233.0 | 248.0 | 102.0 | 15.0 |
| DFT/TZP[h] | 233.8 | 250.0 | 102.8 | 16.2 |
| expt. (MW) | 236.1[i] | n/a | n/a | n/a |

[a] Distances in pm, angles in deg. [b] Standard electron correlation on valence electrons only. [c] All electrons were included in the electron correlation scheme. [d] Weis et al.[53] [e] Wetzel et al.[54] [f] Dickey et al.[50] [g] Malliavin and Coudray.[51] [h] Modisette et al.[52] [i] Derived from $B_e$ rotation constants.[20]

erratic results. Further calculations show that these basis sets behave well when only valence correlation is included but very unpredictably if core correlation is added. This is attributed to the fact that these basis sets are not designed for core correlation as they are of minimal quality in the inner-shell region.[56] Using the correlation-consistent polarized core-valence *n*-tuple $\zeta$ (cc-pCV*n*Z) basis sets for Cl[57,58] and the recently developed equivalent for sodium[59] at quadruple-$\zeta$ level, the monomer distance is further shortened by 0.8 pm, bringing it to within 0.7 pm of the experimental value.

Consistent trends are also seen in calculation results obtained from the literature. With the addition of electron correlation the dimer bonded distance decreases by around 3 pm, although this does not effect the Cl−Na−Cl angle significantly. For the DFT calculations, the shortening of the dimer Na−Cl distance is even more pronounced (by over 6 pm with respect to the non-correlated ab initio value) and a slightly larger Cl−Na−Cl angle is observed.

The Na−Cl distance in the monomer shows a similar trend to that in the dimer, with the addition of electron correlation shortening the bond by around 2−3 pm. The DFT calculations again show a much shorter distance, by around 6 pm.

The difference between the dimer and the monomer Na−Cl distances is reasonably consistent throughout all the calculations (excluding the anomalous results using the cc-pVQZ). Uncorrelated methods give values that vary from 17.4 to 18.3 pm and the introduction of correlation decreases this to a range of 15.3 to 16.6 pm.

Because of the large computational cost associated with the CCSD(T) method and the large core-valence basis sets, the MP2(full)/6-311+G(d) method was used throughout the rest of the study.

**Theoretical Calculations: Vibrational Correction Terms.** Harmonic force fields were computed at the equilibrium geometries for both the monomer and the dimer species at the MP2(full)/6-311+G(d) level to compute the zeroth- and first-order vibrational corrections, for comparison with the EXPRESS method values. The frequencies of the six vibrational modes for the dimer species calculated from this harmonic force field are listed in Table 3 along with the computed value for the monomer. Experimental values are also tabulated.[19,60] All of the calculated stretching frequencies are somewhat high, for exmaple, 1.6% for the monomer and 8−9% for the $B_{2u}$ and $B_{3u}$ dimer modes. The larger discrepancy for the dimer could, in part, result from the effect of the argon matrix used in the experiment.

**TABLE 3: Harmonic Theoretical and Experimental Vibrational Frequencies for the Sodium Chloride Monomer and Dimer Calculated at the MP2(full)/6-311+G(d) Level[a]**

| mode | $\nu_{theo.}$ | $\nu_{expt.}$ |
|---|---|---|
| | Monomer | |
| $A_1$ stretch | 370.5 | 364.6[b] |
| | Dimer | |
| $A_g$ stretch | 279 | |
| $B_{1g}$ stretch | 253 | |
| $B_{2u}$ stretch | 298 | 274[c] |
| $B_{3u}$ stretch | 244 | 226[c] |
| $A_g$ bend | 132 | |
| $B_{1u}$ bend | 96 | 108/115[c] |

[a] Frequencies in $cm^{-1}$. [b] Brumer and Karplus.[19] [c] Martin and Schaber.[60]

The potential-energy curve for the $B_{1u}$ mode of vibration of the dimer is shown in Figure 4 together with plots showing the variation of interatomic distances. The equivalent plots for the other dimer modes and the monomer $A_1$ stretch are shown in Figures S4−S9 (Supporting Information). From Figure 4b we can see that the sodium-chlorine bonded distance increases as the molecule bends. This shows that there is substantial coupling between the $B_{1u}$ bending mode and the $A_g$ stretching mode, which is not possible in a traditional curvilinear approach. The coupling of these two vibrational modes, of different symmetry species, is possible because as the molecule bends ($B_{1u}$) the symmetry drops to $C_{2v}$ and thus both the bending and stretching mode are then of the same symmetry. The interplay of these normal modes in describing this large-amplitude bending motion illustrates how this method has moved beyond the limitations of infinitesimal rectilinear displacements, while still using the basic forms of the normal modes to define the regions of the PES that need to be explored for the EXPRESS method.

For the asymmetric stretching modes ($B_{1g}$, $B_{2u}$, and $B_{3u}$), the potential-energy functions themselves can contain only even terms. (The vibrations are identical either side of equilibrium.) However, the functions relating the potential to the distances do not have this same constraint and this method has also enabled the anharmonicity in these vibrations to be correctly captured. This proved to have an important influence on the final structure.

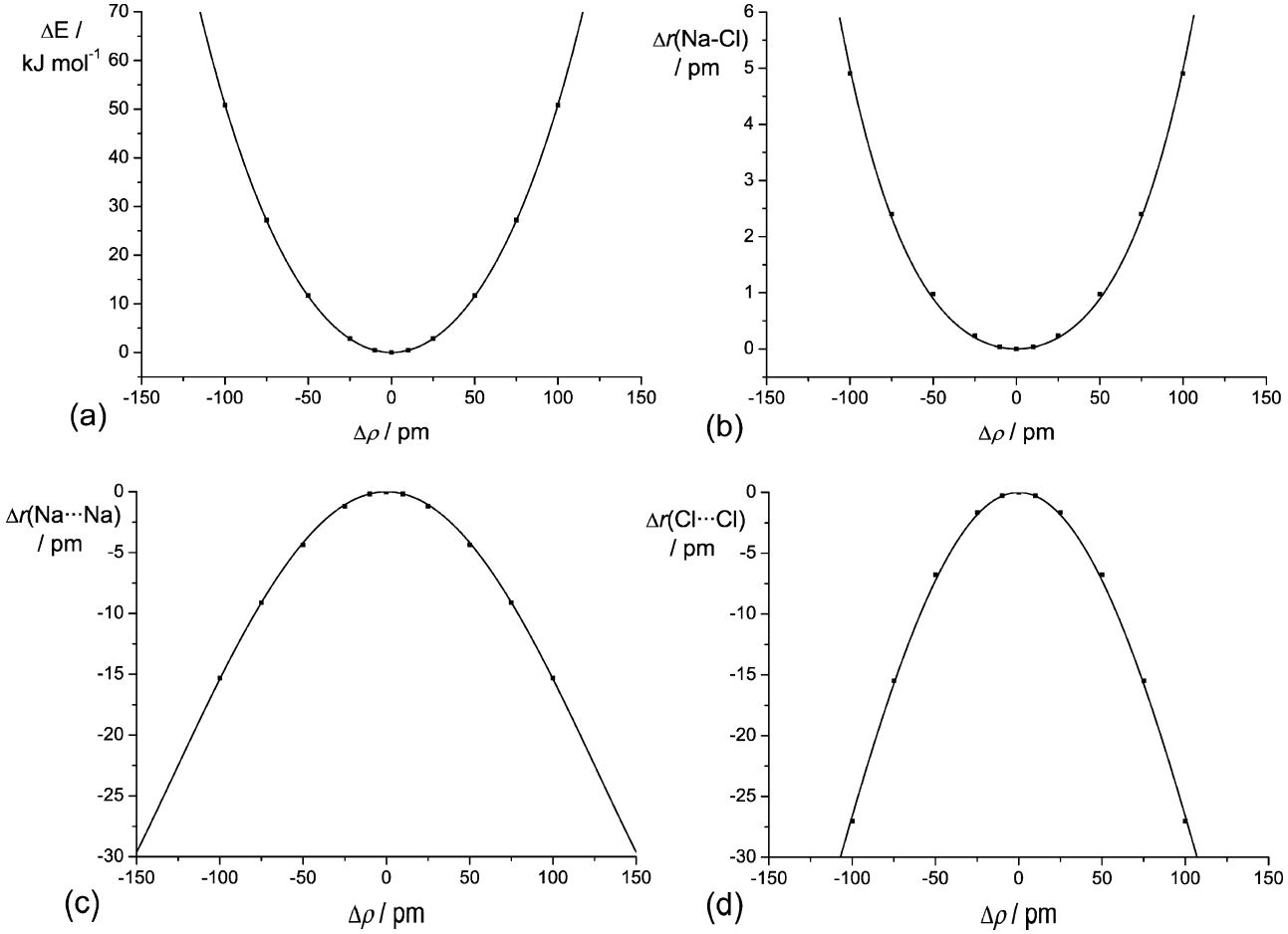


**Figure 4.** Plots of changes in (a) energy, (b) $r$(Na−Cl) bonded distance, (c) $r$(Na···Na) nonbonded distance, and (d) $r$(Cl···Cl) nonbonded distance against change in vibrational mode parameter ($\rho$) for the $B_{1u}$ bending motion.

**TABLE 4: RMS Amplitudes of Vibration ($u$) and Distance Corrections ($r_a - r_e$) for NaCl and $Na_2Cl_2$ Computed Using the EXPRESS Method at 943 K, Centrifugal Distortion Corrections ($\delta r$), and Overall $r_a - r_e$ Corrections[a]**

| distance | | $A_1$ stretch | $A_g$ stretch | $B_{1g}$ stretch | $B_{2u}$ stretch | $B_{3u}$ stretch | $A_g$ bend | $B_{1u}$ bend | total[b] | $\delta r$[c] | overall $(r_a - r_e) + \delta r$ |
|---|---|---|---|---|---|---|---|---|---|---|---|
| | | | | | | Monomer | | | | | |
| Na−Cl | $u$ | 11.36 | | | | | | | 11.36 | | |
| | $r_a - r_e$ | 1.79 | | | | | | | 1.79 | 0.98 | 2.77 |
| | | | | | | Dimer | | | | | |
| Na−Cl | $u$ | | 7.32 | 8.96 | 7.92 | 7.94 | 0.36 | 0.54 | 16.12 | | |
| | $r_a - r_e$ | | 0.79 | 1.06 | 0.85 | 0.86 | 0.19 | 0.29 | 4.04 | 0.59 | 4.63 |
| Na···Na | $u$ | | 9.25 | 0.04 | 3.96 | 0.43 | 22.25 | 2.32 | 24.53 | | |
| | $r_a - r_e$ | | 1.10 | 1.88 | 2.26 | −0.24 | −0.95 | −0.40 | 2.65 | 1.01 | 3.66 |
| Cl···Cl | $u$ | | 11.34 | 4.06 | 1.24 | 4.23 | 18.41 | 4.02 | 22.79 | | |
| | $r_a - r_e$ | | 1.15 | 2.30 | 0.70 | 2.44 | −1.79 | −2.43 | 2.36 | 0.71 | 3.07 |

[a] All values are in pm. [b] For amplitudes see eq 8; for $r_a - r_e$ see eq 9. [c] Calculated from MP2(full)/6-311+G(d) force field using SHRINK.[7,8]

These potential functions and distance variations were then used to calculate the RMS amplitude of vibration ($u^m$) and distance correction terms $[(r_a - r_e)^m]$ using the method described earlier. The explicitly calculated RMS amplitudes of vibration ($u^m$) for each mode of the monomer and dimer, together with the corresponding distance corrections $[(r_a - r_e)^m]$, are listed in Table 4. Also shown are the overall RMS amplitudes of vibration ($u$) and distance corrections ($r_a - r_e$) for each distance, calculated as described above, and the centrifugal distortion terms ($\delta r$) calculated using SHRINK.[7,8]

Comparison of the overall amplitudes of vibration and distance corrections obtained by this method and the equivalent values from previous approaches are shown in Table 5. Our method includes a more complete description of the vibrational motion and implicitly takes into account anharmonicity, to any order.

To define accurately the explicit type of structure that has been obtained from an GED experiment, a systematic nomenclature is required. This will then allow precise comparisons with other experimental and theoretical methods. We propose an extension to the commonly used scheme, which will allow the definition of the level of the force field used ($n$). This can be h when a harmonic force is used, a3 when third derivatives of energy (giving cubic anharmonicity terms) are used, a4 using fourth derivatives, and so forth. The level of the force field term ($n$) should also be augmented with a t if tabulated constants have been used to assess the anharmonicity. As in the present nomenclature, the level of theory ($m$) used in calculating the correction terms is given by 0 for zeroth-order rectilinear corrections, 1 for first-order curvilinear corrections, and so forth. The structure is thus defined using the notation $r_{n,m}$. Examples are included in Table 5.

**TABLE 5: RMS Amplitudes of Vibration and Distance Corrections for NaCl and $Na_2Cl_2$ at 943 K[a]**

| distance | | ASYM ($r_{h0}$)[b] | SHRINK ($r_{h1}$)[c] | SHRINK ($r_{a3t,1}$)[d] | SHRINK ($r_{a3,1}$)[e] | EXPRESS ($r_e$) |
|---|---|---|---|---|---|---|
| | | | Monomer | | | |
| Na−Cl | $u$ | 10.95 | 10.95 | 10.95 | 10.95 | 11.36 |
| | $r_a - r_n$[f] | 0.47 | 0.47 | 2.56 | 2.78 | 2.77 |
| | | | Dimer | | | |
| Na−Cl | $u$ | 15.02 | 15.03 | 15.03 | 15.03 | 16.12 |
| | $r_a - r_n$[f] | 2.09 | 0.20 | 2.98 | 4.77 | 4.63 |
| Na···Na | $u$ | 24.89 | 24.97 | 24.97 | 24.97 | 24.53 |
| | $r_a - r_n$[f] | −0.59 | −2.88 | 0.88 | 3.75 | 3.66 |
| Cl···Cl | $U$ | 22.13 | 22.21 | 22.21 | 22.21 | 22.79 |
| | $r_a - r_n$[f] | −0.47 | −2.43 | 0.62 | 2.89 | 3.07 |

[a] All values are in pm. [b] Obtained from a harmonic force field at MP2(full)/6-311+G(d) level using first-order distance corrections and centrifugal distortion term ($\delta r$). [c] As in footnote *b* but using first-order distance corrections. [d] As in footnote *c* but also including cubic anharmonic effects generated from averaged tabulated values. [e] As in footnote *c* but including cubic anharmonic effects generated using third derivatives of the energy. [f] Correction term from $r_a$ to level of theory used.

Our RMS amplitudes of vibration are similar to those obtained using other approaches. Anharmonic amplitudes of vibration are typically a few percent larger[22] so our slightly larger value for the monomer can be mainly attributed to anharmonic effects that are not taken into account in any of the other approaches. Even though the distance correction terms in the a3t,1 and a3,1 methods include a correction for cubic anharmonic effects, the amplitudes of vibration are still calculated in the harmonic approximation. For the dimer bonded distance, the difference is twice that of the monomer and presumably results from a combination of higher-order modeling of atomic motion as well as anharmonic effects. Cubic anharmonicity should play almost no role in the amplitude of vibration for the nonbonded distances and indeed their differences are much smaller.

Our distance correction ($r_a - r_e$) for the monomer is in good agreement with that obtained from SHRINK using the third derivatives of the energy ($r_{a3,1}$). The Morse oscillator is a very good approximation for a vibrating diatomic and cubic anharmonicity will be the major contributing factor, so such close agreement between the two approaches is encouraging. For comparison, the approach using averaged constants ($r_{a3t,1}$) yielded a Morse anharmonicity ($a_3$) of 11.6 $nm^{-1}$, compared with the spectroscopic value of 13.0 $nm^{-1}$. This is a better value than the typical choice of 20.0 $nm^{-1}$ for a bonded distance,[61] which in this case would result in an anomalously large distance correction (≈50%) for the well-characterized monomer.

Our distance corrections ($r_a - r_e$) for the dimer are markedly different from those obtained using the $r_{h0}$ and $r_{h1}$ approaches because of the large effects of anharmonicity. The harmonic force-field and rectilinear corrections (h,0) used by the ASYM approach give a large positive correction for the bonded distance and a correction of a smaller but negative magnitude for the two nonbonded distances. These correction terms will be largely inaccurate as they dramatically over-correct the bonded distance while under-correcting the nonbonded distances. Increasing the level of sophistication to first-order, curvilinear corrections (h,1) by using the SHRINK program gives a better description of the vibrational motion. This shifts the weight from the bonded to the nonbonded terms, although by neglecting anharmonicity the correction terms for the two nonbonded distances (Na···Na and Cl···Cl) become even more negative, and thus the correction terms become worse. It is essential to include anharmonicity, as seen by the large improvement that is gained simply through the use of tabulated cubic anharmonic constants (a3t,1). This has the effect of making all of the correction terms positive and the magnitude of the bonded correction a factor of 3−5 larger than those for the nonbonded distances. The correction terms are further improved upon by including more accurate cubic anharmonic effects using constants calculated from the third derivatives of the energy. This has the effect of increasing the magnitudes of all of the correction terms. The correction terms calculated by the EXPRESS method ($r_e$) further improve the situation as they take into account anharmonic effects to a higher order and explore a much more extensive region of the PES. However, it is encouraging that the best values obtainable using corrections calculated from conventional force fields ($r_a - r_{a3,1}$) are in reasonable agreement with our distance corrections ($r_a - r_e$).

**TABLE 6: Comparison of RMS Amplitudes of Vibration and Perpendicular Motion Correction Terms Due to the $Na_2Cl_2$ Dimer $B_{1u}$ Out-of-Plane Bending Mode[a]**

| | | ASYM ($r_{h0}$) | SHRINK ($r_{h1}$) | EXPRESS ($r_e$) |
|---|---|---|---|---|
| Na−Cl | $u$ | 0.00 | 0.00 | 0.54 |
| | $r_a - r_n$[b] | 1.71 | 0.00 | 0.29 |
| Na···Na | $u$ | 0.00 | 1.87 | 2.32 |
| | $r_a - r_n$[b] | 0.00 | −2.66 | −0.40 |
| Cl···Cl | $u$ | 0.00 | 1.55 | 4.02 |
| | $r_a - r_n$[b] | 0.00 | −2.20 | −2.43 |

[a] All values in pm. [b] Contribution to overall correction term from $r_a$ to level of theory used, for this mode.

The differences between the three approaches to modeling atomic motion can be best illustrated by considering the $B_{1u}$ out-of-plane bending vibration of the dimer. As this mode has a zero cubic anharmonic component[62] (because all of the interatomic distances must be identical either side of the equilibrium position), we can compare the values obtained from the EXPRESS method to those obtained from the $r_{h0}$ and $r_{h1}$ approaches. These are shown in Table 6.

The zeroth-order approach assumes that the Cl···Cl and Na···Na distances do not change so the Na−Cl bond lengthens by a large amount during the motion, leading to an unrealistically large distance correction for the bonded distance (1.7 pm). The first-order approach effectively fixes the Na−Cl distance, with atoms moving along curved paths. Although this is a better approximation, it overcompensates for the Na···Na nonbonded correction and assumes that the Na−Cl distance does not change (which is not the case). Therefore, neither approach adequately describes the atomic motions in this large-amplitude mode of vibration. Our approach, which involves sampling the PES over an extended region instead of just at the origin, gives values that generally lie between those given by the other two approaches, as expected.

**Gas-Phase Structural Refinements.** In the refinement of the sodium chloride monomer and dimer structures, we have attempted to make use of all available experimental data. The GED data provide information on both structures. In addition, very precise information about the equilibrium monomer bond length is available in the form of rotation constants ($B_e$), obtained from microwave spectroscopy for both $^{23}Na^{35}Cl$ and $^{23}Na^{37}Cl$,[20] details of which are listed in Table 7. The apparent experimental estimated standard deviation (esd) associated with each of the rotational constants was not large enough to account for the discrepancies between the determined $r_e$ structures for the two isotopomers. This may indicate the breakdown of the traditional Born−Oppenheimer PES, but this phenomenon is not of concern at the level of accuracy obtained by GED. Therefore, the esd for these measurements was increased beyond

**TABLE 7: $B_e$ Constants[a]**

| | $B_e$ | $r_e$[b] | $B_e$ used in GED refinement |
|---|---|---|---|
| $^{23}Na^{35}Cl$ | 6537.36521(37) | 2.36079485(7) | 6537.3652(30) |
| $^{23}Na^{37}Cl$ | 6397.28111(78) | 2.36079378(14) | 6397.2811(30) |

[a] Rotation constants in MHz, distances in pm. [b] Derived from $B_e$ rotation constants.[20]

**TABLE 8: Refined $r_e$ Vapor Structures and Composition for NaCl Vapor at 943 K[a]**

| | | $r_e$ (exptl) | $r_e$ (theory)[b] | restraint |
|---|---|---|---|---|
| | Independent Parameters | | | |
| $p_1$ | $r(Na-Cl)_{monomer}$ | 236.0794(4) | 236.8 | |
| $p_2$ | $r(Na-Cl)_{dimer}$ | 253.4(9) | 253.3 | |
| $p_3$ | ∠ClNaCl | 102.7(11) | 101.8 | |
| $p_4$ | $F_{dimer}$ | 0.27(2) | | |
| | Dependent Parameters | | | |
| $d_1$ | r(Na···Na) | 316.5(43) | 319.6 | |
| $d_2$ | r(Cl···Cl) | 395.7(32) | 393.2 | |
| $d_3$ | $\Delta r(Na-Cl)$ [c] | 17.3(9) | 16.6 | |
| $d_4$ | $B_e$ $^{23}Na^{35}Cl$ | 6537.3688(19) | | 6537.3652(30) |
| $d_5$ | $B_e$ $^{23}Na^{37}Cl$ | 6397.2788(19) | | 6397.2811(30) |

[a] Distances in pm, angles in deg, and rotational constants in MHz. Numbers in parenthesis are estimate standard deviations. [b] Theoretical results from MP2 calculations using all-electron correlation and CVQZ for sodium and cc-pCVQZ basis set for chlorine. [c] Change in bonded distance on moving from the monomer to dimer.

the quoted experimental value to allow the $r_e$ structure to be geometrically consistent.

The rotational constants were introduced as extra information in the form of flexible restraints, calculated using physical constants and atomic masses available from the National Institute of Standards and Technology.[63] This is possible in the *ed@ed* structural refinement program as it allows non-GED data to be employed as additional data during the least-squares refinement process. Restraints derived from theoretical data can also be applied using the SARACEN method[1−3] and these were used to restrain some vibrational amplitudes or their ratios to calculated values.

Four independent parameters (Table 8) were used to describe the structure and composition of the sodium chloride vapor. Parameter $p_1$ describes the bond length, $r$(Na−Cl), for the monomer, $p_2$ is the dimer bond length $r$(Na−Cl), $p_3$ is ∠(Cl−Na−Cl), and $p_4$ is the proportion of NaCl units existing as dimer in the vapor ($F_d$), as defined in eq 10. Previous studies[22] have defined the fractional amount of dimer in terms of a mole fraction, but it is more appropriate to use our approach, as it is the total number of monomer units that remains constant.

$$F_d = \frac{2m_d}{m_m + 2m_d} \qquad (10)$$

where $m_m$ and $m_d$ are the relative numbers of moles of monomer and dimer, respectively.

Together with the four independent parameters, the RMS amplitudes of vibration were refined. As the bonded distances for the monomer and dimer cannot be resolved in the electron-diffraction experiment, the ratio of the amplitudes of vibration was restrained using values calculated from the EXPRESS method. Any other amplitudes that could not be refined sensibly were subject to a SARACEN restraint, with the uncertainty taken to be 10% of the computed value. Starting values for the refining geometrical parameters were taken from an ab initio calculation using the MP2 method, applying the correlation to all electrons, using the cc-pCVQZ basis for chlorine and CVQZ for sodium.

**TABLE 9: Refined RMS Amplitudes of Vibration ($u$), Associated $r_a$ Distances, and Corresponding Values Calculated from Theory[a]**

| | | $r_a$ | $u_{(exptl)}$ | $u_{(calcd)}$ | restraint/ constraint |
|---|---|---|---|---|---|
| $u_1$ | $r(Na-Cl)_{monomer}$[b] | 238.8494(5) | 10.6(3) | 11.4 | |
| $u_2$ | $r(Na-Cl)_{dimer}$[b] | 256.6(9) | 16.2(4) | 16.1 | |
| $u_3$ | r(Na···Na) | 316.5(44) | 24.6(21) | 24.5 | 24.5(25) |
| $u_4$ | r(Cl···Cl) | 398.1(30) | 20.1(14) | 22.8 | 22.8(23) |

[a] Distances in pm. [b] $u_1/u_2$ restrained to the calculated ratio of 0.703(50).

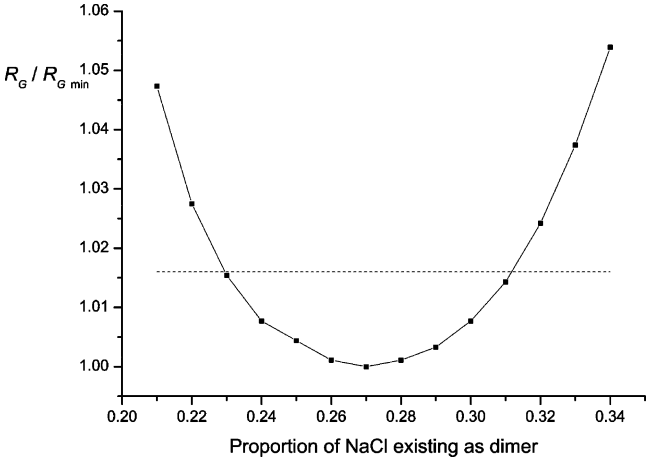


**Figure 5.** Variation of R factor with amount of $Na_2Cl_2$ dimer at 943 K. The dashed line marks the 95% confidence limit.

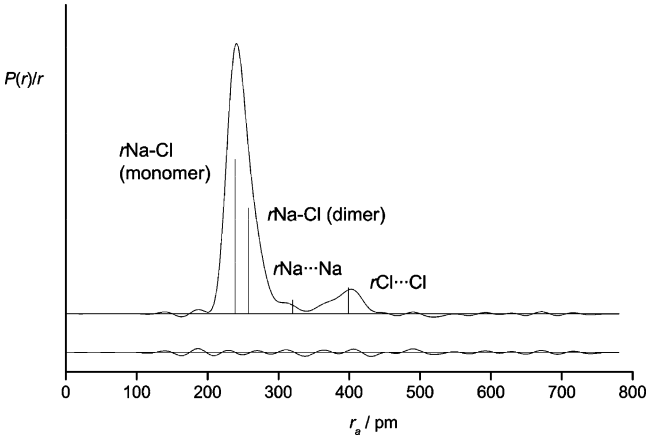


**Figure 6.** Experimental and difference (experimental−theoretical) radial-distribution curves, $P(r)/r$, for sodium chloride vapor at 943 K. Before Fourier inversion the data were multiplied by $s$ exp(−0.000 $02s^2$)/($Z_{Cl}$ − ×c4$_{Cl}$)($Z_{Na}$ − ×c4$_{Na}$).

The starting values for the RMS amplitudes of vibration ($u$) and distance corrections ($k$) were calculated using the EXPRESS method, as described above.

The refinement parameters, their final refined values, and all flexible restraints are shown in Table 8. The refined amplitudes and associated $r_a$ distances are listed in Table 9.

The proportion of vapor existing as dimer ($p_4$) was fixed at various values and the refinement process repeated. The variation of $R_G$ with the proportion of dimer is shown in Figure 5 along with the 95% confidence limit (≈2$\sigma$) calculated using Hamilton's tables.[64] This leads to a final value for the proportion of dimer of 0.27(4) with an $R_G$ factor of 0.091. The final molecular intensity curve is depicted in Figure 6 and final radial distribution curve in Figure 7.

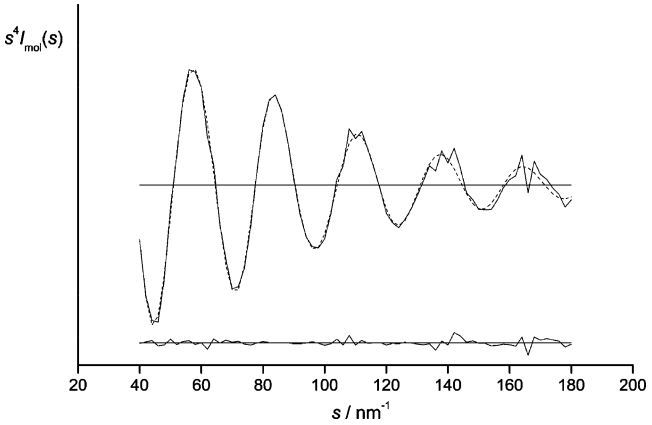


**Figure 7.** Molecular scattering intensities and difference curve for sodium chloride vapor at 943 K. Solid line, experimental data; dashed line, theoretical data; lower solid line, difference curve.

The fit between experimental and theoretical scattering, as determined by the $R_G$ factor, is reasonably good, considering the noise due to the high temperature of the experiment, especially above $s = 100$ nm$^{-1}$, and is a significant improvement over the original fit.[22] The radial-distribution difference curve has a much more uniform distribution than those obtained in previous studies,[22,65] suggesting that the residual is noise rather than indicating a problem with any structural parameter.

Allowances for multiple-scattering effects[66] have not been included in this study. Multiple scattering is an important consideration for molecules containing heavy atoms, especially when a triplet forms an angle close to 90°.[67,68] In the present case, although the angles are not far from 90°, preliminary work we have conducted has shown that the effect of this is negligible. However, multiple-scattering effects will have a more significant effect for heavier alkali halide dimers, and we are developing methods to deal with them. Sensitive mass-spectrometric studies on other alkali halides have shown the presence of larger oligomers (such as trimers and tetramers), but their vapor pressures are several orders of magnitude smaller than that of the dimer.[69,70] More recently a mass-spectrometric study of vaporization fluxes from alkali halide single crystals detected no presence of trimer for sodium chloride.[71]

Table 10 compares the results of our refinement using the EXPRESS method with the original analysis by Mawhorter et al.,[22] as well as a study by Frischknecht and Mawhorter[62] combining an ASYM analysis ($r_{h0}$) with retrospective cubic anharmonic corrections, obtained from a Morse oscillator model, to bonded distances. Results from a refinement that we have performed using amplitudes ($u$) and distance corrections ($r_a - r_{a3,1}$) generated using SHRINK and anharmonic constants from the third derivatives of the energy are also tabulated, together with theoretical results obtained using the MP2(full)/CVQZ/cc-pCVQZ method, for comparison.

The EXPRESS method ($r_e$ structure) reduces the standard deviations for all the refined parameters when compared to both the previous study by Mawhorter et al.[22] and Frischknecht and Mawhorter[62] and the refinement using the best corrections generated from SHRINK ($r_{a3,1}$). The improved accuracy of the refined structure using the EXPRESS method (compared to the one obtained using SHRINK's vibrational correction terms) is a consequence of the improved description of the vibrations. The larger improvement when compared to previous studies can be attributed to the improved vibrational corrections, as well as the use of the microwave data for the monomer and the flexible restraints of the SARACEN method, which consequently provided the ability to refine all parameters and RMS amplitudes of vibration simultaneously. The improvement in the refinement is also highlighted by the absence of any systematic (non-noise) errors in the radial distribution curve (Figure 7).

When compared to our highest level ab initio calculation [MP2(full)//CVQZ/cc-pCVQZ] the monomer and dimer bonded distances are both calculated to be too long (the monomer by 0.7 pm, the dimer by 0.2 pm). While experiment and theory do agree for the dimer (within experimental error), a better comparison is the change in bonded distance going from the monomer to the dimer, $\Delta r$(Na−Cl). At this level of theory the difference is 16.6 pm, which is within one standard deviation of our experimentally determined value of 17.3(9) pm. This calculated difference should be more accurate than absolute values as systematic errors in the calculations of both the monomer and the dimer will tend to cancel. Frischknecht and Mawhorter's value of 15.5 is reasonable because of the inclusion of anharmonicity and the near equivalence of the linear normal mode and curvilinear displacements for this particular geometry.[62] Although the best SHRINK calculation also gives good agreement for the dimer structure, the combination of the improved distance corrections and the use of anharmonic RMS amplitudes of vibration ($u$) from the EXPRESS method give improved accuracy of the determined parameters, an improved fit and a better agreement between theory and experiment for the more accurately calculated change in bonded distance, $\Delta r$(Na−Cl) (one esd for our method compared with two esd's for the a3,1 analysis).

## Conclusion

Equilibrium structures have been obtained from GED experiments. This has been achieved by generating explicit distance corrections that directly relate GED structures to the $r_e$ structures from ab initio calculations as well as other experiments. These are generated from the analysis of those parts of the ab initio PES that correspond to the modes of vibration of the molecule. These correction terms therefore include all of the effects of anharmonicity to a high order and more accurately describe atomic motion, especially in modes with large-amplitude modes of vibration.

This technique has been successfully applied to the GED structural refinement of sodium chloride vapor at 943 K, to give

**TABLE 10: Comparison of Experimental Results from Different Methods of Analysis[a]**

| parameter | ref 22 ($r_a$) | ref 62 ($r_{h0} + A_3$)[b] | SHRINK ($r_{a3,1}$) | EXPRESS ($r_e$) | theory[c] ($r_e$) |
|---|---|---|---|---|---|
| $r$(Na−Cl)$_{monomer}$ | 238.8(4)[d] | 235.9(4)[d] | 236.0794(4) | 236.0794(4) | 236.8 |
| $r$(Na−Cl)$_{dimer}$ | 258.4(17)[d] | 251.4(20)[d] | 254.2(9) | 253.4(9) | 253.6 |
| ∠(ClNaCl) | 101.4(12)[d] | 101.7(14)[d] | 102.5(12) | 102.7(11) | 101.8 |
| $\Delta r$(Na−Cl) | 19.6 | 15.5 | 18.1(9) | 17.3(9) | 16.6 |
| $F_{dimer}$ | 0.28(6)[d,e] | | 0.24(2)[d] | 0.27(2)[d] | |
| $R_G$ | 0.112 | | 0.093 | 0.091 | |

[a] Distances in pm, angles in deg. [b] $r_{h0}$ approach with anharmonic corrections to bonded distances. [c] Calculated using MP2(full) and using the CVQZ basis set for sodium and cc-pCVQZ for chlorine. [d] Uncertainties converted to 1$\sigma$. [e] Converted from quoted mole fraction to proportion of NaCl units existing as dimer (see eq 10).

accurate determinations of the experimental equilibrium structures of both the monomer and dimer, and of the amount of vapor existing as dimer. The structures obtained make use of all the available information (GED, MW, and ab initio calculations) and the calculated vibrational correction terms provide small but nevertheless important perturbations to the structure obtained purely by experimental means. Nevertheless, the final structure is still derived primarily from experimental data. These results for the dimer and the monomer−dimer expansion now give very good agreement with high-level ab initio theory, within experimental error.

Of key importance to the accuracy of this study was the inclusion of anharmonic effects. By using the best corrections obtainable from the program SHRINK, which includes an assessment of cubic anharmonic effects from the third derivatives of the energy ($r_{a3,1}$), comparable accuracy can be obtained for this simple system, where the EXPRESS method has been limited to exploring 1D slices of the PES that correspond to the normal modes of vibration. The EXPRESS method also has the capability to explore more complicated systems with multiple coupled large-amplitude and/or highly anharmonic modes, for which more extensive regions of multidimensional surfaces may need to be explored. We plan to apply the method to increasingly complex structural problems of this nature.

**Acknowledgment.** P.D.M. is grateful to the School of Chemistry (University of Edinburgh) for funding a studentship and would like to thank S. Wilsey (Service Manager, NSCCS) for her help and advice. A.R.T. and P.T.B. thank the EPSRC for funding (Grants GR/R17768 and GR/K4411), and R.J.M. gratefully acknowledges the support of the Mellon Foundation and the Donors of the Petroleum Research Fund, administered by the American Chemical Society, for partial support of this research.

**Supporting Information Available:** Correlation matrix for refinement. Coordinates of refined $r_e$ structure. Graphs of change in energy, change in $r$(Na−Cl) bond length, change in $r$(Na···Na) nonbonded distance, and change in $r$(Cl···Cl) nonbonded distance against vibrational mode parameter for the $A_g$, $B_{1g}$, $B_{2u}$, and $B_{3u}$ stretching modes and the $A_g$ bending mode of the $Na_2Cl_2$ dimer. Graph of change in energy against vibrational mode parameter for the $A_1$ stretching mode of the NaCl monomer. Fitting functions and coefficients for all the vibrational modes. Derived correction terms from the EXPRESS method. Tables of ab initio geometries and energies. Detailed refinement results obtained using the $r_{a3,1}$ analysis. This material is available free of charge via the Internet at http://pubs.acs.org.

## References and Notes

(1) Brain, P. T.; Morrison, C. A.; Parsons, S.; Rankin, D. W. H. *J. Chem. Soc., Dalton Trans.* **1996**, 4589−96.
(2) Mitzel, N. W.; Rankin, D. W. H. *Dalton Trans.* **2003**, 3650−62.
(3) Blake, A. J.; Brain, P. T.; McNab, H.; Miller, J.; Morrison, C. A.; Parsons, S.; Rankin, D. W. H.; Robertson, H. E.; Smart, B. A. *J. Phys. Chem.* **1996**, *100*, 12280−7.
(4) Hinchley, S. L.; Haddow, M. F.; Rankin, D. W. H. *Dalton Trans.* **2004**, 384−91.
(5) Jensen, P. *J. Mol. Spectrosc.* **1988**, *128*, 478−501.
(6) Jensen, P. *J. Chem. Soc., Faraday Trans. 2* **1988**, *84*, 1315−40.
(7) Sipachev, V. A. *THEOCHEM* **1985**, *22*, 143−51.
(8) Sipachev, V. A. In *Advances in Molecular Structure Research*; Hargittai, I. H. M., Ed.; JAI: Greenwich, 1999; Vol. 5, pp 323−71.
(9) Hedberg, L.; Mills, I. M. *J. Mol. Spectrosc.* **1993**, *160*, 117−42.
(10) Hedberg, L.; Mills, I. M. *J. Mol. Spectrosc.* **2000**, *203*, 82−95.
(11) Clabo, D. A., Jr.; Allen, W. D.; Remington, R. B.; Yamaguchi, Y.; Schaefer, H. F., III. *Chem. Phys.* **1988**, *123*, 187−239.
(12) Sipachev, V. A. *Struct. Chem.* **2000**, *11*, 167−72.
(13) Toerring, T.; Biermann, S.; Hoeft, J.; Mawhorter, R.; Cave, R. J.; Szemenyei, C. *J. Chem. Phys.* **1996**, *104*, 8032−42.
(14) Kruckeberg, S.; Schooss, D.; Maier-Borst, M.; Parks, J. H. *Phys. Rev. Lett.* **2000**, *85*, 4494−7.
(15) Dally, A. J.; Bloomfield, L. A. *Phys. Rev. Lett.* **2003**, *90*, 063401/1−063401/4.
(16) Meyer, G.; Repp, J.; Zophel, S.; Braun, K.-F.; Hla, S. W.; Folsch, S.; Bartels, L.; Moresco, F.; Rieder, K. H. *Single Molecules* **2000**, *1*, 79−86.
(17) Maxwell, L. R.; Hendricks, S. B.; Mosley, V. M. *Phys. Rev.* **1937**, *52*, 968−72.
(18) Friedman, L. *J. Chem. Phys.* **1955**, *23*, 477−82.
(19) Brumer, P.; Karplus, M. *J. Chem. Phys.* **1973**, *58*, 3903−18.
(20) Caris, M.; Lewen, F.; Winnewisser, G. *Z. Naturforsch., A.: Phys. Sci.* **2002**, *57*, 663−8.
(21) Clouser, P. L.; Gordy, W. *Phys. Rev.* **1964**, *134*, 863−70.
(22) Mawhorter, R. J.; Fink, M.; Hartley, J. G. *J. Chem. Phys.* **1985**, *83*, 4418−26.
(23) Liescheski, P. B.; Rankin, D. W. H. *J. Mol. Struct.* **1989**, *196*, 1−19.
(24) Bastiansen, O.; Traetteberg, M. *Acta Crystallogr.* **1960**, *13*, 1108.
(25) Breed, H.; Bastiansen, O.; Almenningen, A. *Acta Crystallogr.* **1960**, *13*, 1108.
(26) Morino, Y. *Acta Crystallogr.* **1960**, *13*, 1107.
(27) Wilson, E. B.; Decius, J. C.; Cross, P. C. *Molecular Vibrations*; McGraw-Hill: New York, 1955.
(28) Frisch, M. J.; Trucks, G. W.; Schlegel, H. B.; Scuseria, G. E.; Robb, M. A.; Cheeseman, J. R.; Montgomery, J. A., Jr.; Vreven, T.; Kudin, K. N.; Burant, J. C.; Millam, J. M.; Iyengar, S. S.; Tomasi, J.; Barone, V.; Mennucci, B.; Cossi, M.; Scalmani, G.; Rega, N.; Petersson, G. A.; Nakatsuji, H.; Hada, M.; Ehara, M.; Toyota, K.; Fukuda, R.; Hasegawa, J.; Ishida, M.; Nakajima, T.; Honda, Y.; Kitao, O.; Nakai, H.; Klene, M.; Li, X.; Knox, J. E.; Hratchian, H. P.; Cross, J. B.; Bakken, V.; Adamo, C.; Jaramillo, J.; Gomperts, R.; Stratmann, R. E.; Yazyev, O.; Austin, A. J.; Cammi, R.; Pomelli, C.; Ochterski, J. W.; Ayala, P. Y.; Morokuma, K.; Voth, G. A.; Salvador, P.; Dannenberg, J. J.; Zakrzewski, V. G.; Dapprich, S.; Daniels, A. D.; Strain, M. C.; Farkas, O.; Malick, D. K.; Rabuck, A. D.; Raghavachari, K.; Foresman, J. B.; Ortiz, J. V.; Cui, Q.; Baboul, A. G.; Clifford, S.; Cioslowski, J.; Stefanov, B. B.; Liu, G.; Liashenko, A.; Piskorz, P.; Komaromi, I.; Martin, R. L.; Fox, D. J.; Keith, T.; Al-Laham, M. A.; Peng, C. Y.; Nanayakkara, A.; Challacombe, M.; Gill, P. M. W.; Johnson, B.; Chen, W.; Wong, M. W.; Gonzalez, C.; Pople, J. A. *Gaussian 03*, revision C.01; Gaussian, Inc.: Wallingford, CT, 2004.
(29) Møller, C.; Plesset, M. S. *Phys. Rev.* **1934**, *46*, 618−22.
(30) Saebo, S.; Almlof, J. *Chem. Phys. Lett.* **1989**, *154*, 83−9.
(31) Head-Gordon, M.; Head-Gordon, T. *Chem. Phys. Lett.* **1994**, *220*, 122−8.
(32) Frisch, M. J.; Head-Gordon, M.; Pople, J. A. *Chem. Phys. Lett.* **1990**, *166*, 281−9.
(33) Frisch, M. J.; Head-Gordon, M.; Pople, J. A. *Chem. Phys. Lett.* **1990**, *166*, 275−80.
(34) Head-Gordon, M.; Pople, J. A.; Frisch, M. J. *Chem. Phys. Lett.* **1988**, *153*, 503−6.
(35) Pople, J. A.; Krishnan, R.; Schlegel, H. B.; Binkley, J. S. *Int. J. Quantum Chem.* **1978**, *14*, 545−60.
(36) Cizek, J. *Adv. Chem. Phys.* **1969**, *14*, 35−89.
(37) Purvis, G. D., III; Bartlett, R. J. *J. Chem. Phys.* **1982**, *76*, 1910−8.
(38) Scuseria, G. E.; Janssen, C. L.; Schaefer, H. F., III. *J. Chem. Phys.* **1988**, *89*, 7382−7.
(39) Scuseria, G. E.; Schaefer, H. F., III. *J. Chem. Phys.* **1989**, *90*, 3700−3.
(40) Pople, J. A.; Head-Gordon, M.; Raghavachari, K. *J. Chem. Phys.* **1987**, *87*, 5968−75.
(41) Bartlett, R. J.; Purvis, G. D. *Int. J. Quantum Chem.* **1978**, *14*, 561−81.
(42) EPSRC National Service for Computational Chemistry Software. URL: http://www.nsccs.ac.uk.
(43) McLean, A. D.; Chandler, G. S. *J. Chem. Phys.* **1980**, *72*, 5639−48.
(44) Krishnan, R.; Binkley, J. S.; Seeger, R.; Pople, J. A. *J. Chem. Phys.* **1980**, *72*, 650−4.
(45) Clark, T.; Chandrasekhar, J.; Spitznagel, G. W.; Schleyer, P. v. R. *J. Comput. Chem.* **1983**, *4*, 294−301.
(46) Frisch, M. J.; Pople, J. A.; Binkley, J. S. *J. Chem. Phys.* **1984**, *80*, 3265−9.
(47) Laane, J. *J. Phys. Chem.* **1991**, *95*, 9246−9.
(48) Hinchley, S. L.; Robertson, H. E.; Borisenko, K. B.; Turner, A. R.; Johnston, B. F.; Rankin, D. W. H.; Ahmadian, M.; Jones, J. N.; Cowley, A. H. *Dalton Trans.* **2004**, 2469−76.
(49) Ross, A. W.; Fink, M.; Hilderbrandt, R. In *International Tables for Crystallography*; Wilson, A. J. C., Ed.; Kluwer Academic Publishers: Dordrecht, The Netherlands, 1992; Vol. C, p 245.
(50) Dickey, R. P.; Maurice, D.; Cave, R. J.; Mawhorter, R. *J. Chem. Phys.* **1993**, *98*, 2182−90.

(51) Malliavin, M. J.; Coudray, C. *J. Chem. Phys.* **1997**, *106*, 2323−30.
(52) Modisette, J.; Lou, L.; Nordlander, P. *J. Chem. Phys.* **1994**, *101*, 8903−7.
(53) Weis, P.; Ochsenfeld, C.; Ahlrichs, R.; Kappes, M. M. *J. Chem. Phys.* **1992**, *97*, 2553−60.
(54) Wetzel, T. L.; Moran, T. F.; Borkman, R. F. *J. Phys. Chem.* **1994**, *98*, 10042−7.
(55) Lee, B.; Lee, S. *J. Korean Chem. Soc.* **2000**, *44*, 190−193.
(56) Woon, D. E.; Dunning, T. H., Jr. *J. Chem. Phys.* **1995**, *103*, 4572−85.
(57) Woon, D. E.; Dunning, T. H., Jr. *J. Chem. Phys.* **1993**, *98*, 1358−71.
(58) Peterson, K. A.; Dunning, T. H., Jr. *J. Chem. Phys.* **2002**, *117*, 10548−10560.
(59) Iron, M. A.; Oren, M.; Martin, J. M. L. *Mol. Phys.* **2003**, *101*, 1345−1361.
(60) Martin, T. P.; Schaber, H. *J. Chem. Phys.* **1978**, *68*, 4299−303.
(61) Robiette, A. G. *Molecular Structure by Diffraction Methods*; The Chemical Society: London, 1973; Vol. 1.
(62) Frischknecht, A. L.; Mawhorter, R. J. *Mol. Phys.* **1998**, *93*, 583−592.
(63) National Institute of Standards and Technology. URL: http://www.physics.nist.gov.
(64) Hamilton, W. C. *Acta Crystallogr.* **1965**, *18*, 502−10.
(65) Miki, H.; Kakumoto, K.; Ino, T.; Kodera, S.; Kakinoki, J. *Acta Crystallogr., Sect. A* **1980**, *A36*, 96−103.
(66) Miller, B. R.; Bartell, L. S. *J. Chem. Phys.* **1980**, *72*, 800−7.
(67) Richardson, A. D.; Hedberg, K.; Lucier, G. M. *Inorg. Chem.* **2000**, *39*, 2787−93.
(68) Gundersen, G.; Hedberg, K.; Strand, T. G. *J. Chem. Phys.* **1978**, *68*, 3548−52.
(69) Viswanathan, R.; Hilpert, K. *Ber. Bunsen-Ges.* **1984**, *88*, 125−31.
(70) Hilpert, K. *Ber. Bunsen-Ges.* **1984**, *88*, 132−9.
(71) Butman, M. F.; Smirnov, A. A.; Kudin, L. S.; Munir, Z. A. *Surf. Sci.* **2000**, *458*, 106−112.